Q-Array: R&D towards superconducting targets for CEνNS

Magnificent CEνNS 2024

Wouter Van De Pontseele

Massachusetts Institute of Technology

June 13, 2024

wvdp@mit.edu

Ricochet aims to build a **low-energy reactor neutrino observatory** at the ILL reactor in France.

- A double cryogenic detector payload: **Cryocube** (Germanium crystals) and **Q-Array** (Superconducting crystals).
- Modular **kg-scale** detector
- Complementary technologies with **Discrimination between electronic** (ER) and **nuclear recoil** (NR)
- Active **R&D** with the first phase started neutrino data taking in **early 2024**.

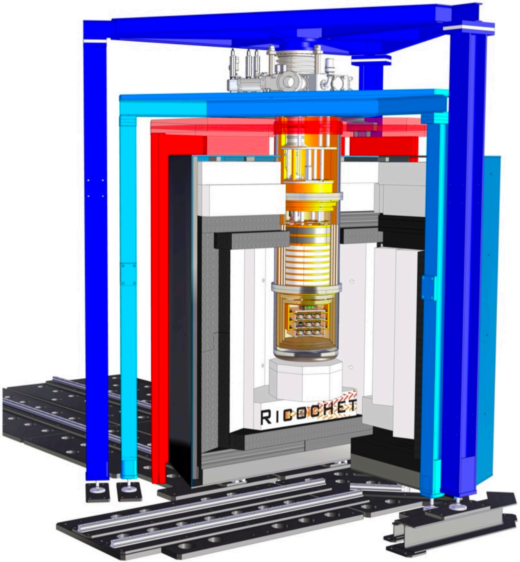

iP2i Les 2 Infinis Lyon
IJCLab Irène Joliot-Curie Laboratoire de Physique des 2 Infinis
ILL Neutrons for Society
LPSC Grenoble
MIT
Joint Institute for Nuclear Research
Néel institut
Northwestern University
University of Massachusetts Amherst
University of Oxford
University of Toronto
Argonne National Laboratory
Lincoln Laboratory Massachusetts Institute of Technology

Q-Array: Superconducting crystals for CEνNS

Hardware R&D

Superconducting crystals (Zn, Al, and Sn) as absorbers.

Transition edge sensor “chips” as sensors.

Cryogenic **RF-SQUID resonators**.

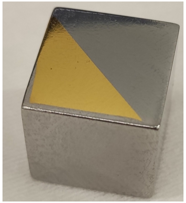

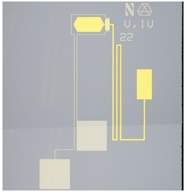

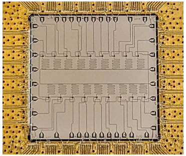

Advantage / Goal

Access to **lower thresholds**; timing as recoil discriminator

Modular fast readout; **standardised fabrication** process

Multiplexed readout, scalable and reduced heatload.

The **detectors and readout chain** envisaged can be broken up into four parts that are **designed, fabricated and tested individually**.
Each of these has **applications beyond CEνNS** and is pursued by many quantum computing and fundamental physics projects.

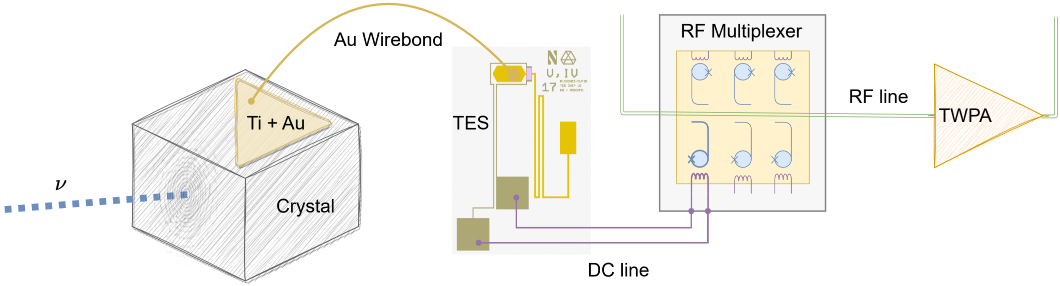

- Dielectrics (like Si and Ge)
  - Ionisation with energy gap of $\mathcal{O}(1\,\mathrm{eV})$.
  - Athermal phonons below the gap are long-lived.

$\rightarrow E_{recoil} \gtrsim 10\,\mathrm{eV}$: **Energy goes into heat and ionisation, PID**

$\rightarrow E_{recoil} \lesssim 10\,\mathrm{eV}$: **Heat only, no ionisation, no PID**

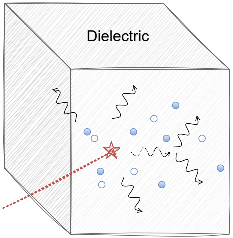

- Superconductors
  - Debye energy > 2Δ gap.
    Athermal phonons above the gap have a short mean free path and create quasi-particles.
    Quasi-particles eventually recombine into Cooper pairs.

$\rightarrow$ **All energy eventually converted to heat**

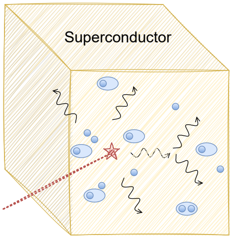

- Dielectrics (like Si and Ge)
  - Ionisation with energy gap of $\mathcal{O}(1\,\text{eV})$.
  - Athermal phonons below the gap are long-lived.

$\rightarrow E_{recoil} \gtrsim 10\,\text{eV}$: **Energy goes into heat and ionisation, PID**

$\rightarrow E_{recoil} \lesssim 10\,\text{eV}$: **Heat only, no ionisation, no PID**

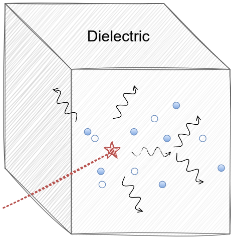

- Superconductors
  - Debye energy > 2Δ gap.
    Athermal phonons above the gap have a short mean free path and create quasi-particles.
    Quasi-particles eventually recombine into Cooper pairs.

$\rightarrow$ **All energy eventually converted to heat**

$\rightarrow$ **Athermal phonons and quasi-particles** might have **electronic/nuclear recoil** discrimination.

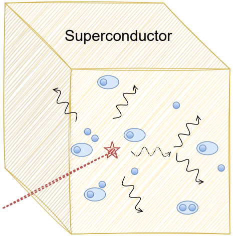

Collect and concentrate athermal excitations into the sensing region

- Deposit a superconducting layer with $\Delta_{trap} < \Delta_{absorber}$.
- QPs shed off phonons and are trapped.
- Athermal phonons with $2\Delta_{trap} < \Omega < 2\Delta_{absorber}$ will create QPs.
- **Selective collection** possible: **Dielectric layer** (Oxides) creates a barrier for QPs but not for phonons.

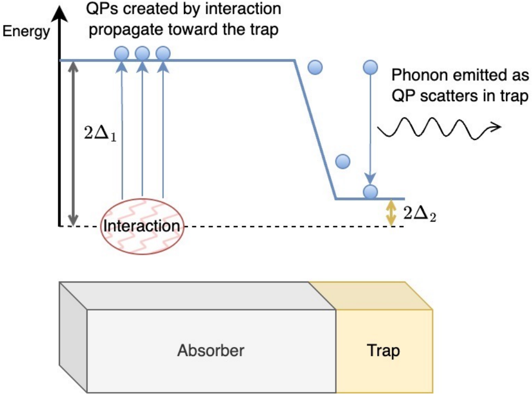

Collect and concentrate athermal excitations into the sensing region

- Deposit a superconducting layer with $\Delta_{trap} < \Delta_{absorber}$.
- QPs shed off phonons and are trapped.
- Athermal phonons with $2\Delta_{trap} < \Omega < 2\Delta_{absorber}$ will create QPs.
- **Selective collection** possible: **Dielectric layer** (Oxides) creates a barrier for QPs but not for phonons.

Q-array: **thermalise the trapped excitations in a gold layer** with small heat capacity.

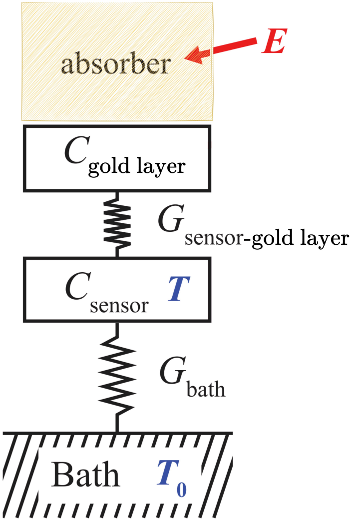

thin **superconductoing film** at an **intermediate** resistance between its **normal and superconducting state**.

- **Self-stabilising** using negative electro-thermal feedback if voltage biased **after energy pulse**: $T_{TES} \uparrow \Rightarrow R_{TES} \uparrow \Rightarrow$ Joule heating $\downarrow \Rightarrow T_{TES} \downarrow$

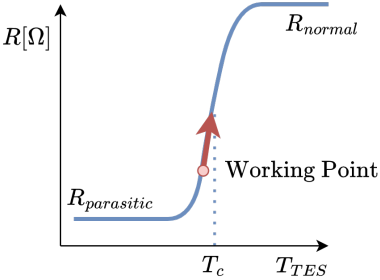

thin **superconductoing film** at an **intermediate** resistance between its **normal and superconducting state**.

- **Self-stabilising** using negative electro-thermal feedback if voltage biased **after energy pulse**: $T_{TES} \uparrow \Rightarrow R_{TES} \uparrow \Rightarrow$ Joule heating $\downarrow \Rightarrow T_{TES} \downarrow$
- Ricochet uses **Manganese doped Aluminium** fabricated at Argonne National Lab.

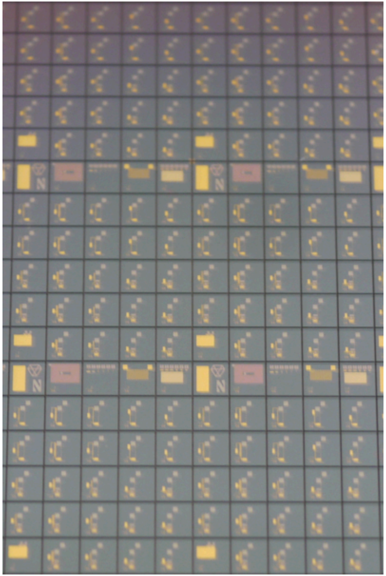

thin **superconductoing film** at an **intermediate** resistance between its **normal and superconducting state**.

- **Self-stabilising** using negative electro-thermal feedback if voltage biased **after energy pulse**: $T_{TES} \uparrow \Rightarrow R_{TES} \uparrow \Rightarrow$ Joule heating $\downarrow \Rightarrow T_{TES} \downarrow$
- Ricochet uses **Manganese doped Aluminium** fabricated at Argonne National Lab.
- T_c of AlMn can be predictably increased **after fabrication** by heating.

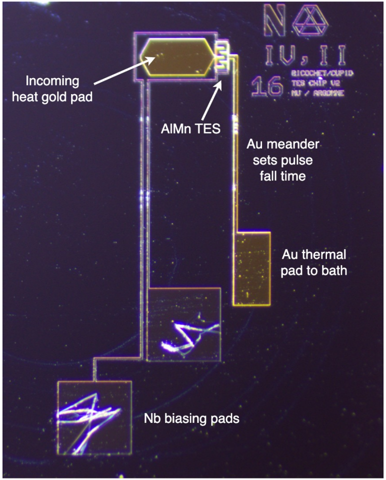

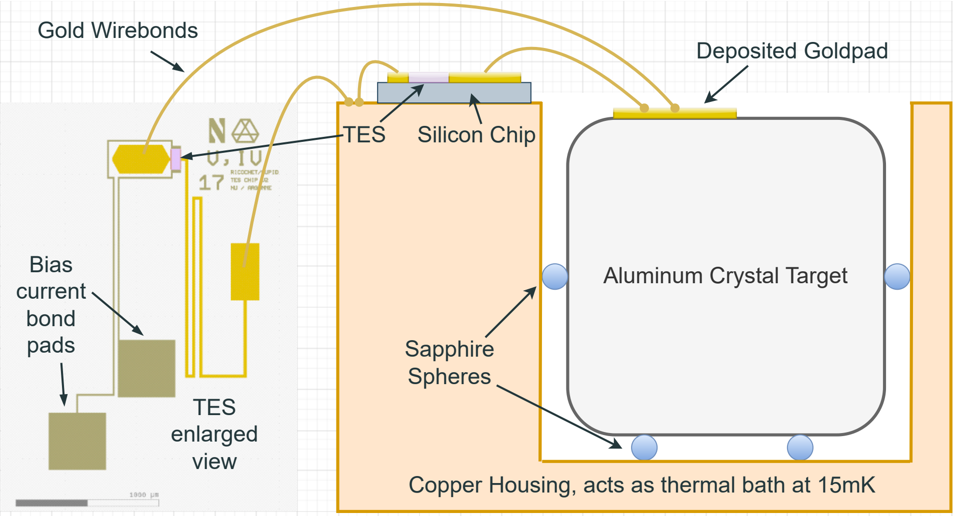
Gold Wirebonds
Deposited Goldpad
TES
Silicon Chip
Bias current bond pads
TES enlarged view
Aluminum Crystal Target
Sapphire Spheres
Copper Housing, acts as thermal bath at 15mK

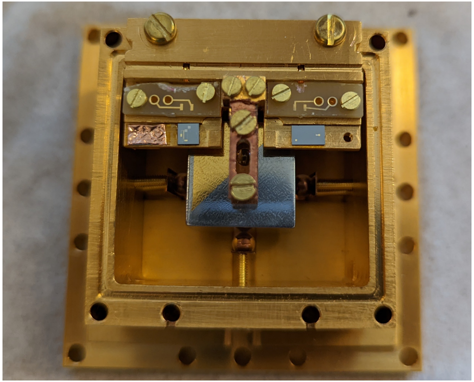

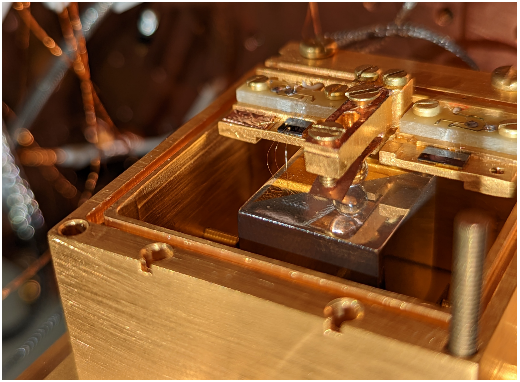

Prototyping boxes deployed at MIT, UMASS, Fermilab testing **modular TES-crystal readout**.

Crystal with TES readout: Pulse reconstruction and modelling

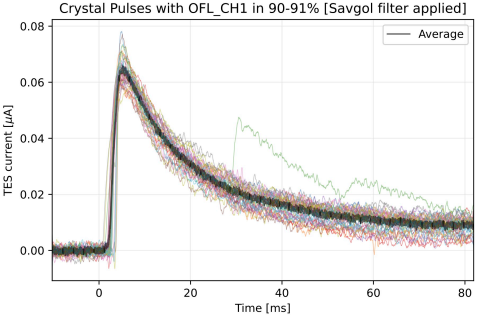

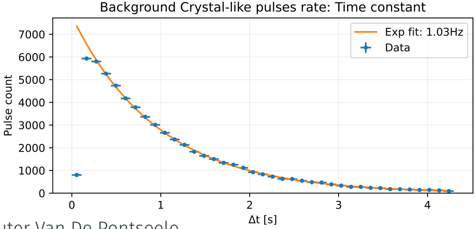

- **Pulses observed with different time constants** in Zinc and Alumunium crystals.
- TES-Crystal **electro-thermal pulse shape modelling**.
- **simulate the energy deposits** of **radioactive sources** into to crystal with GEANT4.

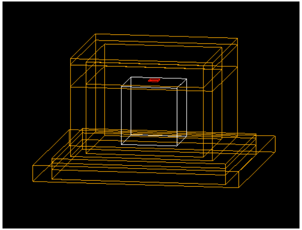

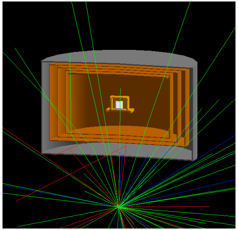

Unique Facility

- 10 mK dilution refrigerator
- Class 10,000 clean room
- 107 m rock, ≈300 $m_{w.e.}$
- $\mathcal{O}(100)$ dru

Germanium and Tin crystal collecting pulses!

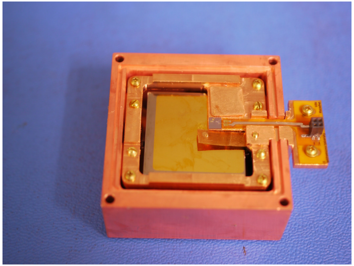

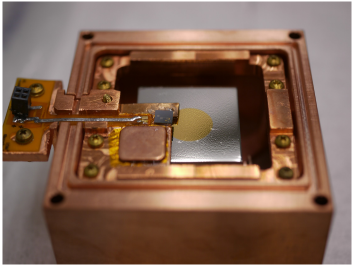

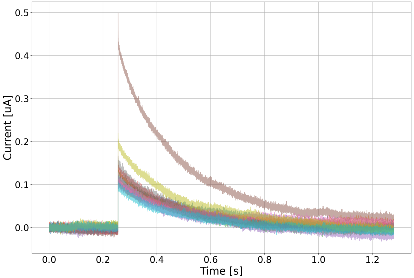

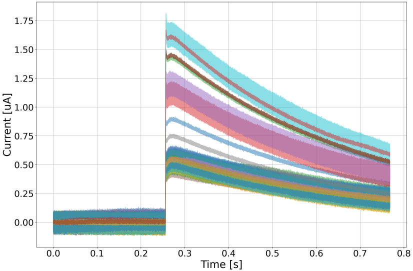

Cryogenic frequency multiplexing

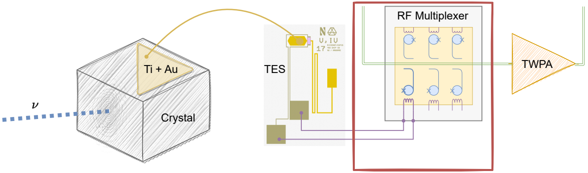

Working principle: Encode **low frequency** TES **signals** into **microwave resonators**.

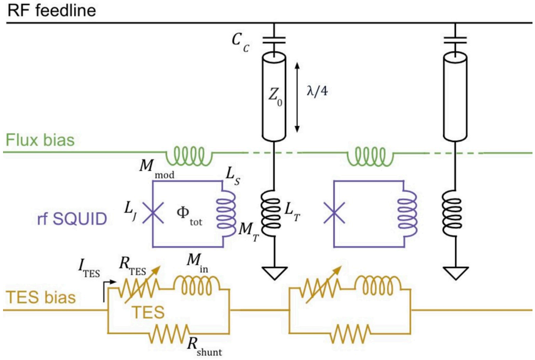

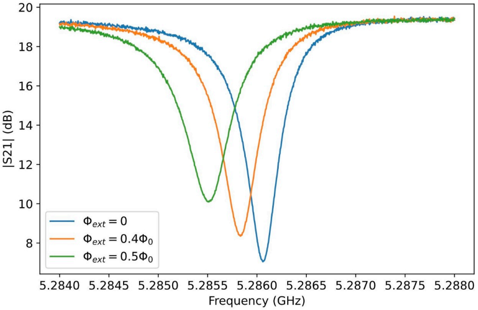

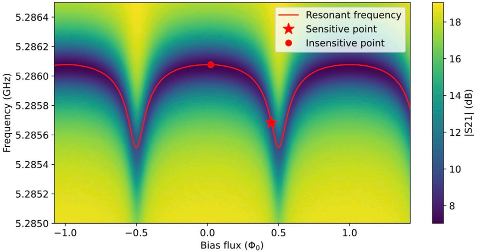

Microwave multiplexing designed at MIT for RICOCHET

Resonator devices fabricated at Lincoln Laboratory with **high quality factor** molecular-beam epitaxy (MBE) **Al** base metal and Dolan-style Josephson junctions.”

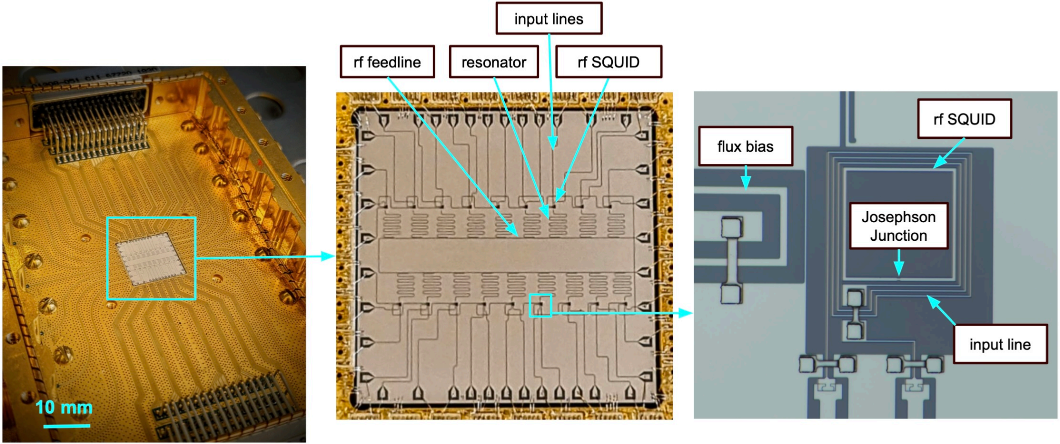

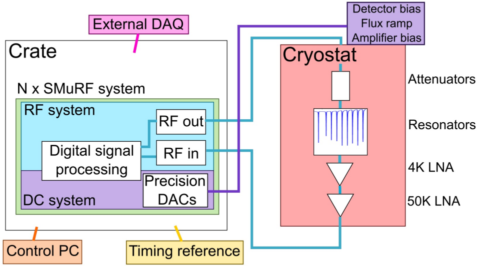

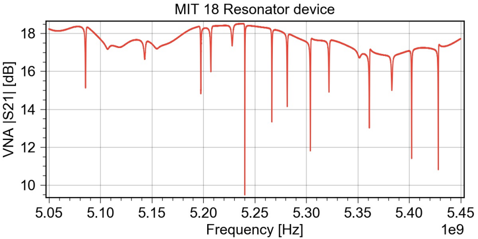

Fully **automated** readout using **SLAC Microresonator RF (SMuRF)** Electronics.

- **Complexity** moved to **warm electronics**.
- FPGA-based resonator tone-tracking.
- DAQ with TES-pulse demodulation.
- Capable of up to $\mathcal{O}(1000)$ channels.

Test setup at MIT with 18 resonator device.

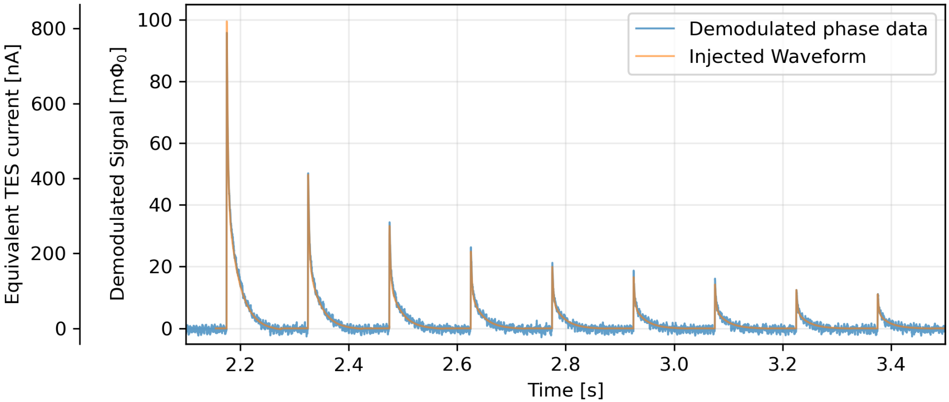

Injected signal-like pulse train reconstructed with MIT multiplexer and SMuRF electronics!

Conclusion & Outlook

The Ricochet Experiment — Talk by Nicolas MARTINI

- CEνNS **cross-section** using cryogenic detectors
- Reactor data-taking **started in 2024**, scaling-up ongoing

Superconducting Crystal and TES Measurements

- **Pulses** in prototype **superconducting Zn/Al/Sn** crystals
- Energy **calibration using sources** in progress

Q-Array RF multiplexed Readout

- Optimised **18-resonator devices fabricated**
- R&D into **high dynamic range quantum amps**

RICOCHET
A Coherent Neutrino Scattering Program

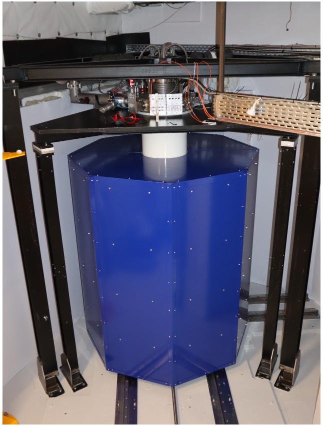

Thank you!

WVDP@MIT.EDU

Special thanks to
RICOCHET collaboration,
MIT Laboratory for Nuclear Science,
MIT Lincoln Laboratories, MIT.Nano & SLAC
J. Formaggio, P. Harrington, J. Yang and K. O'Brien

REFERENCES

Ricochet. Results from a prototype tes detector for the ricochet experiment, 2023.

Cyndia Yu, Zeeshan Ahmed, Josef C. Frisch, Shawn W. Henderson, Max Silva-Feaver, Kam Arnold, David Brown, Jake Connors, Ari J. Cukierman, J. Mitch D'Ewart, Bradley J. Dober, John E. Dusatko, Gunther Haller, Ryan Herbst, Gene C. Hilton, Johannes Hubmayr, Kent D. Irwin, Chao-Lin Kuo, John A. B. Mates, Larry Ruckman, Joel Ullom, Leila Vale, Daniel D. Van Winkle, Jesus Vasquez, and Edward Young. SLAC microresonator RF (SMuRF) electronics: A tone-tracking readout system for superconducting microwave resonator arrays. *Review of Scientific Instruments*, 94(1):014712, jan 2023. doi:10.1063/5.0125084. URL `https://doi.org/10.1063%2F5.0125084`.

Yonit Hochberg, Matt Pyle, Yue Zhao, and Kathryn M. Zurek. Detecting superlight dark matter with fermi-degenerate materials. *Journal of High Energy Physics*, 2016(8), aug 2016. doi:10.1007/jhep08(2016)057. URL *https://doi.org/10.1007%2Fjhep08%282016%29057*.

JPA

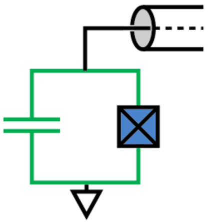

- Few spatial modes – **Cavity** style
- Near **ideal quantum efficiency**
- **Small bandwidth** of $\mathcal{O}$**(10 MHz)**.

JTWPA

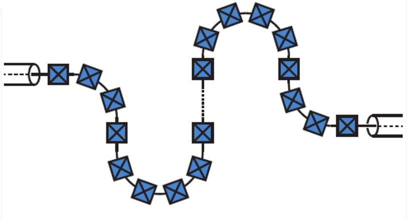

- **Cell size** $< \lambda$
  $\Rightarrow$ Create nonlinear meta-material.
- Many spatial modes
  $\Rightarrow$ **Transmission line** behaviour.
- Up to $\mathcal{O}$**(3 GHz) bandwidth**.

The Ricochet Experiment: ILL reactor at Grenoble

Reactor power: 58 MW
Enriched: 93 % ^{235}U
Diameter ≈40 cm
Distance from core: ≈9 m
Overburden ≈14 $m_{w.e.}$

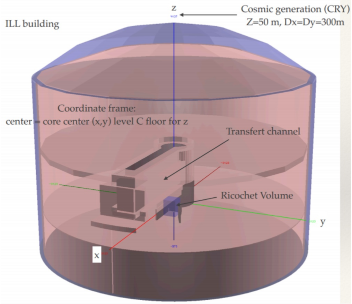

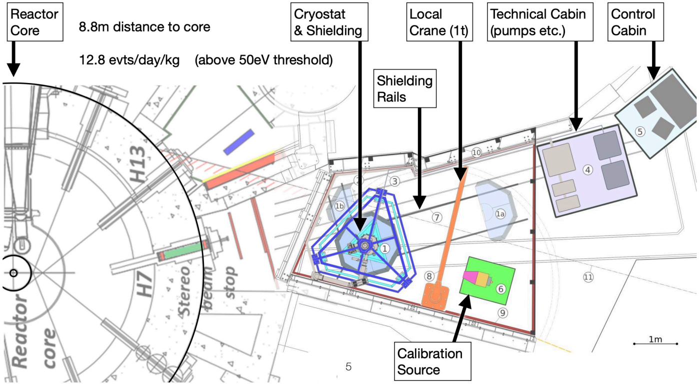

Highly similar setup to HFIR at slightly lower power

SPLENDOR: Search for Particles of Light Dark Matter with Narrow-gap Semiconductors

WHY NARROW BANDGAPS?

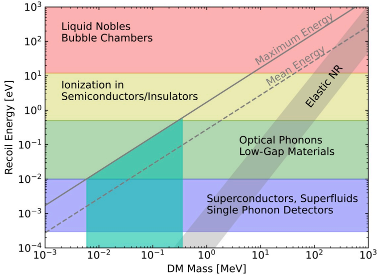

Recoil energy scales and detection technology. Adapted from arXiv:2203.08297

- Light dark matter searches via DM-electron scattering are fundamentally limited by bandgap
- With novel materials with small (order 10-100 meV) bandgaps, we can search for sub-MeV fermionic dark matter and sub-eV bosonic dark matter

IN-HOUSE MATERIALS GROWTH

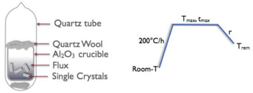

Flux Growth

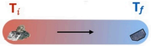

Chemical Vapor Transport

SOME CANDIDATE MATERIALS

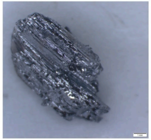

$Eu_5In_2Sb_6$

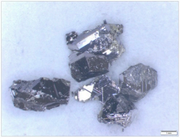

$EuZn_2P_2$

by Samuel Watkins

Superconducting crystal fabrication

Vertical Bridgman growth: slow cooling of molten material by moving from a hot zone into a cold one.

- Cut and Polished into $\mathcal{O}$(cm) cubes.
- Al (N=27), Zn (N=64) or Sn (N=120).

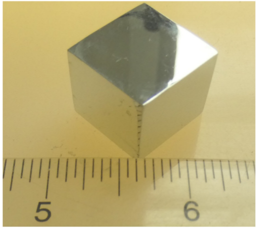

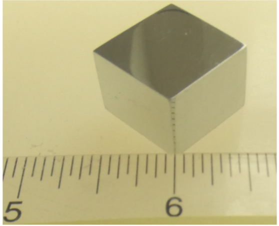

Vertical Bridgman growth: slow cooling of molten material by moving from a hot zone into a cold one.

- Cut and Polished into $\mathcal{O}$(cm) cubes.
- Al (N=27), Zn (N=64) or Sn (N=120).

Gold deposit to collect phonons and/or trap QPs

- **Ti adhesion/trapping layer**
- Gold trapping/thermisation layer $\mathcal{O}(1\,\mu\text{m})$.
- **Natural oxide** impedes quasi-particle trapping.

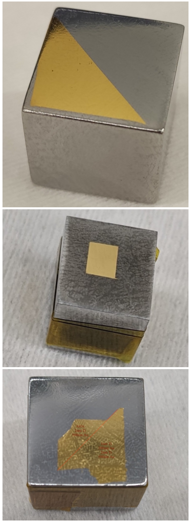

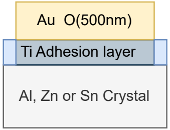

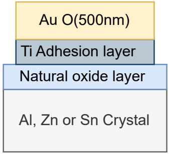

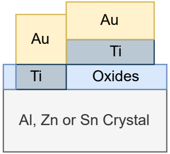

TES and Al crystal measurements: Pulses

- **Prototype** data taking:
  Radioactive sources for calibration:
  - Co60: 1.17 MeV γ, 1.33 MeV γ
  - Ba133: 0.36 MeV γ
  - AmBe: 4.4 MeV γ and neutrons 0 to 8 MeV
- **Pulse** analysis using matched filters.
- Pulses observed with Zn and Al crystals at MIT and 100 m underground at Fermilab

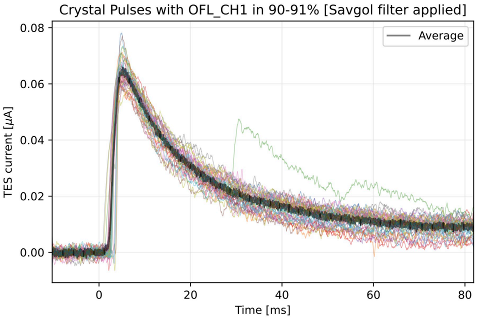

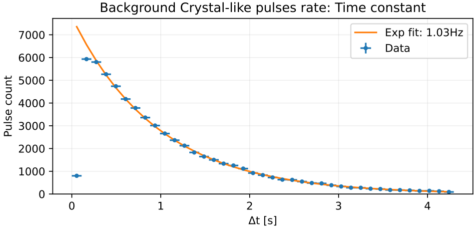

- **Prototype** data taking:
  Radioactive sources for calibration:
  - Co60: 1.17 MeV γ, 1.33 MeV γ
  - Ba133: 0.36 MeV γ
  - AmBe: 4.4 MeV γ and neutrons 0 to 8 MeV
- **Pulse** analysis using matched filters.
- Pulses observed with Zn and Al crystals at MIT and 100 m underground at Fermilab

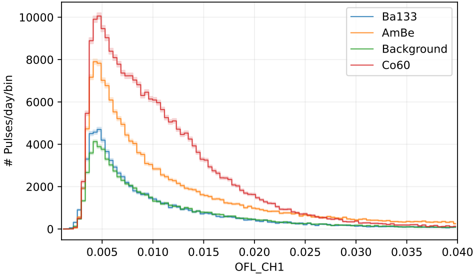

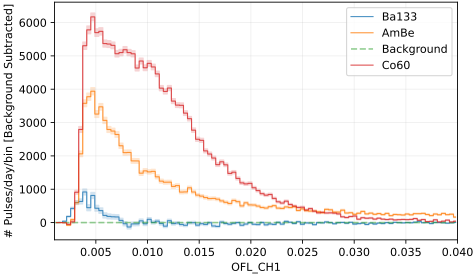

TES and Al crystal measurements: Pulses

- **Prototype** data taking:
  Radioactive sources for calibration:
  - Co60: 1.17 MeV γ, 1.33 MeV γ
  - Ba133: 0.36 MeV γ
  - AmBe: 4.4 MeV γ and neutrons 0 to 8 MeV
- **Pulse** analysis using matched filters.
- Pulses observed with Zn and Al crystals at MIT and 100 m underground at Fermilab

Next generation crystals and boxes cold!

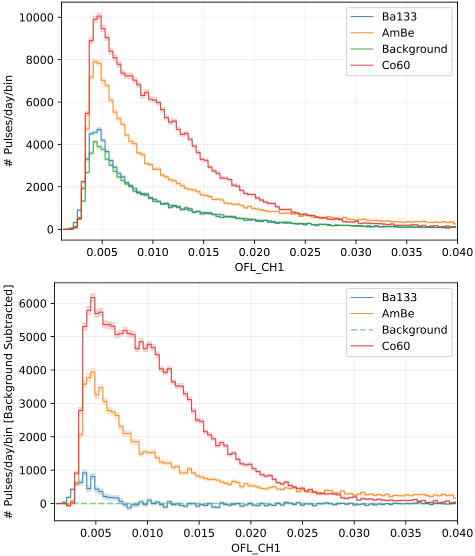

Resonant frequency depends on the current through the inductance.

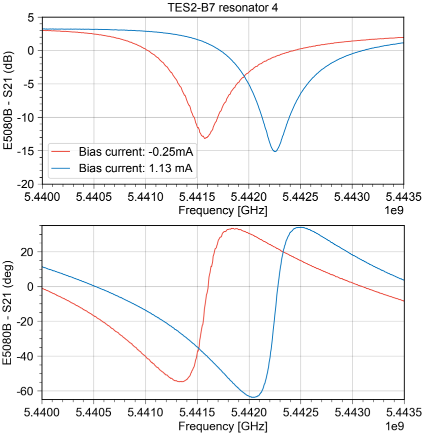

- **Periodicity** enables determination of flux quantum Φ_0.

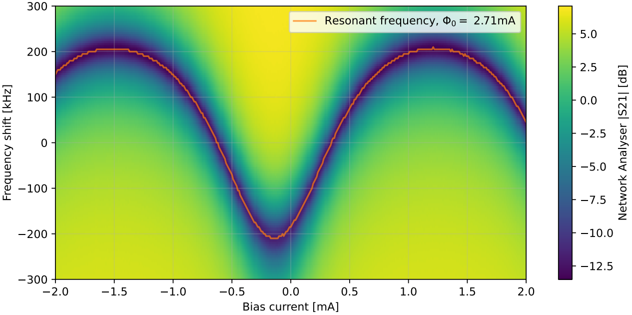

Resonant frequency depends on the current through the inductance.

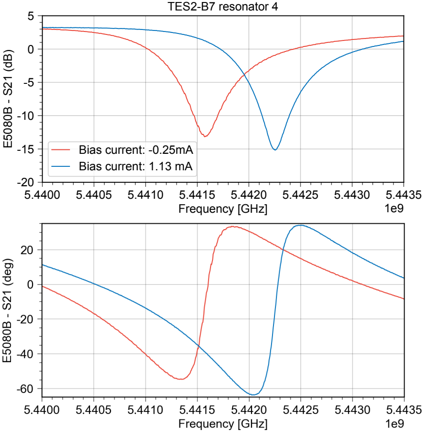

- **Periodicity** enables determination of flux quantum Φ_0.
- **Sensitivity** of $\approx 1\mu\Phi_0/\sqrt{\mathrm{Hz}}$ measured, Translates to $\approx 8\mathrm{pA}/\sqrt{\mathrm{Hz}}$ TES current noise.

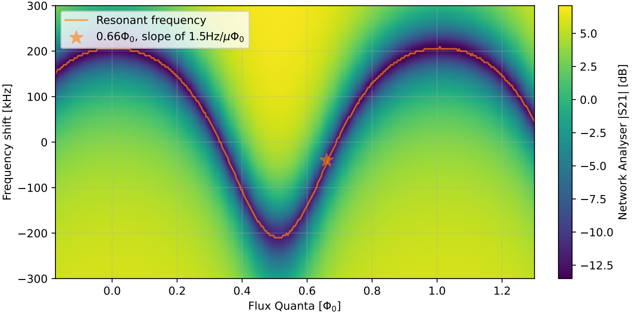

Comparison of design and measured parameters

- |S21| fit to extract resonant frequency, internal and external quality factor.
- Fit of resonant frequency as a function of SQUID flux and probe tone power to obtain inductances.

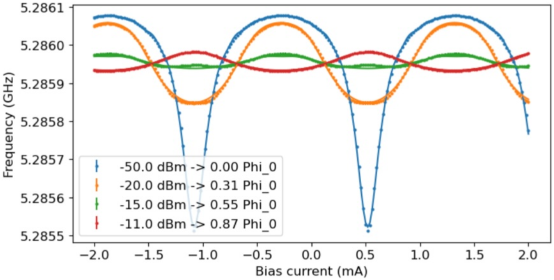

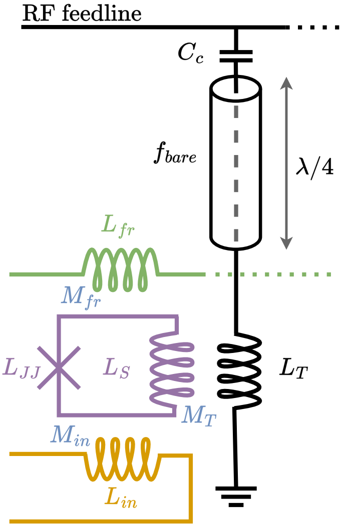

Al crystal with TES Pulses: Shape characterisation — by Mingyu Li

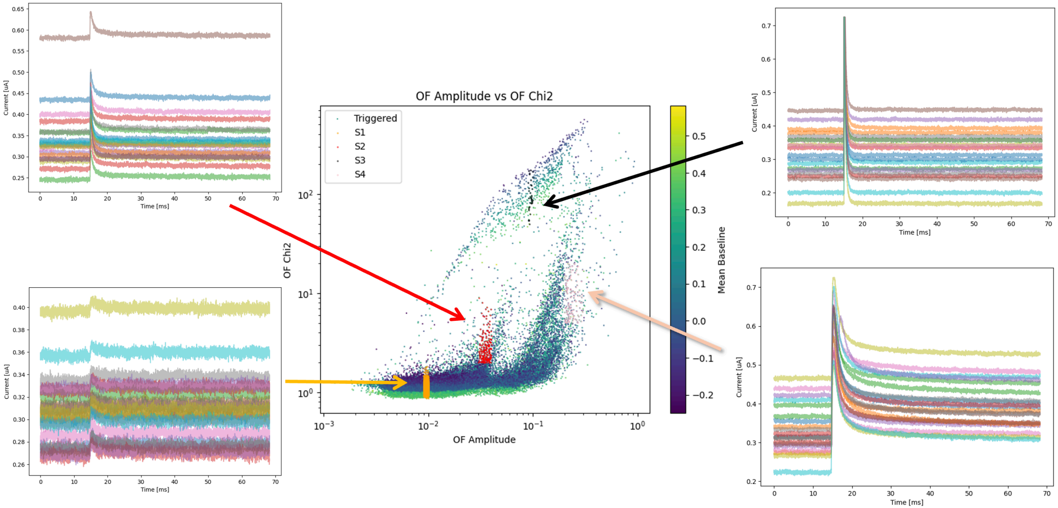

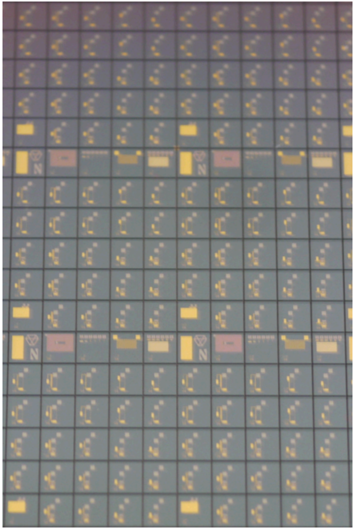

Manganese doped Aluminum (AlMn) with a Ti and Au caption layer TES fabricated at Argonne National Laboratory

Fabrication

- **adding additional gold structures** possible using either etching or liftoff.
- Aimed at **transition temperature** 17 mK to 70 mK.

Performance

- Higher **thermal conductivity** compared to Ir/Pt bilayer.
- T_c of AlMn can be predictably increased **after fabrication** by heating.

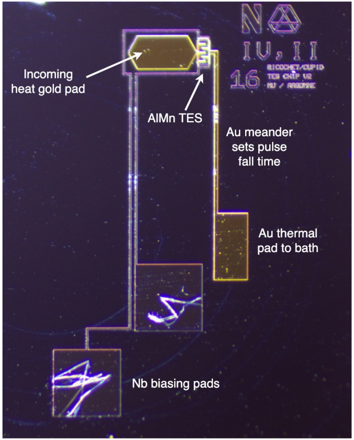

Manganese doped Aluminum (AlMn) with a Ti and Au caption layer TES fabricated at Argonne National Laboratory

Fabrication

- **adding additional gold structures** possible using either etching or liftoff.
- Aimed at **transition temperature** 17 mK to 70 mK.

Performance

- Higher **thermal conductivity** compared to Ir/Pt bilayer.
- T_c of AlMn can be predictably increased **after fabrication** by heating.

Josephson Travelling Wave Parametric Amplifier (JTWPA)

Lowering the multiplexing noise floor further by going beyond HEMTs… **Quantum Amplifiers**!

Signal amplification by exchanging **pump power into signal** and idler tone with Josephson junctions as a non-linear element.

- **Transmission device**. $\mathcal{O}(1000)$ cells.
- Up to $\boldsymbol{\mathcal{O}}$**(3 GHz) bandwidth** with **20 dB gain**.
- Designed by Kevin O’Brien’s group at MIT, fabrication at Lincoln Laboratory.

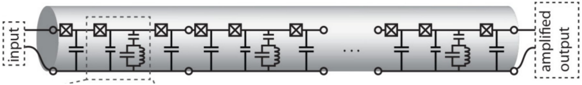

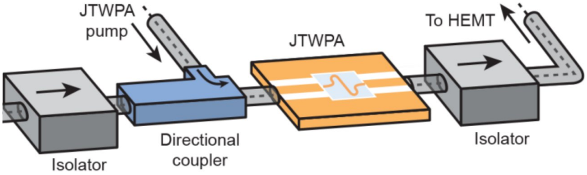

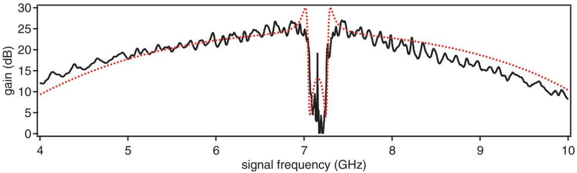

Why?

- **Mass/size per detector limited** to the $\mathcal{O}$(cm) scale to keep heat capacity small and have **ballistic phonon and QP propagation** [Hochberg et al., 2016].
- **rates scale with detector mass**.
- Experiments aim at $\mathcal{O}$(100) **channels**.
- **Minimise heat load** and cold-stage complexity.

Why?

- **Mass/size per detector limited** to the $\mathcal{O}$(cm) scale to keep heat capacity small and have **ballistic phonon and QP propagation** [Hochberg et al., 2016].
- **rates scale with detector mass**.
- Experiments aim at $\mathcal{O}$(100) **channels**.
- **Minimise heat load**
  and cold-stage complexity.

How?

- Time domain multiplexing
- Frequency domain multiplexing
- Code domain multiplexing

Why?

- **Mass/size per detector limited** to the $\mathcal{O}$(cm) scale to keep heat capacity small and have **ballistic phonon and QP propagation** [Hochberg et al., 2016].
- **rates scale with detector mass**.
- Experiments aim at $\mathcal{O}(100)$ **channels**.
- **Minimise heat load** and cold-stage complexity.

How?

- Time domain multiplexing
  Noise scales with $\sqrt{\#\text{channels}}$.
- Frequency domain multiplexing
  Limited by single SQUID bandwidth of $\mathcal{O}$(MHz).
- Code domain multiplexing
  TES-SQUID wiring complexity scales as $(\#\text{channels})^2$.

Why?

- **Mass/size per detector limited** to the $\mathcal{O}$(cm) scale to keep heat capacity small and have **ballistic phonon and QP propagation** [Hochberg et al., 2016].
- **rates scale with detector mass**.
- Experiments aim at $\mathcal{O}$(100) **channels**.
- **Minimise heat load** and cold-stage complexity.

How?

- Time domain multiplexing
  Noise scales with $\sqrt{\#\text{channels}}$.
- Frequency domain multiplexing
  Limited by single SQUID bandwidth of $\mathcal{O}$(MHz).
- Code domain multiplexing
  TES-SQUID wiring complexity scales as $(\#\text{channels})^2$.

$\rightarrow$ Microwave-SQUID multiplexing (μMUX)